

the K vacancies are mainly produced at internuclear distances $R \gtrsim R_K$. Hence the fraction γ of K vacancies transferred to the $1s\sigma$ orbital can be assumed to be constant, and $P_{1s\sigma} = \gamma P_K$ is also constant for $b < R_K$. The assumption is in close agreement to the parametrization of $P_{1s\sigma}$ used in Ref. 5.

¹⁶E. J. McGuire, Phys. Rev. A **2**, 273 (1970).

¹⁷B. Müller, K. Smith, and W. Greiner, Phys. Lett. **49B**, 219 (1974).

¹⁸B. Müller, private communication.

¹⁹F. Bell *et al.*, Phys. Rev. Lett. **35**, 841 (1975).

²⁰I. Tserruya *et al.*, to be published.

²¹We thank K. Smith for performing these calculations for us.

Observation of Two-Photon Optical Nutation and Free-Induction Decay

Michael M. T. Loy

IBM Thomas J. Watson Research Center, Yorktown Heights, New York 10598

(Received 14 April 1976)

The observation of two-photon optical nutation and free-induction decay is reported. The experimental result, on a two-photon transition in NH_3 with all relevant parameters known, is shown to be in quantitative agreement with the prediction of the two-photon vector model.

This Letter reports the first experimental observation of two-photon nutation and free-induction decay (FID), the two-photon analogs of well-known one-photon coherent effects.¹ Following the initial work of Hartmann,² there has been much interest in two-photon coherent effects, both theoretically³⁻⁶ and experimentally.⁷⁻⁹ In the experiment to be reported here, all relevant parameters of the NH_3 two-photon transition are known and the observation can be quantitatively compared with theory. The agreement is shown to be excellent. In addition, the crucial roles of the optical Stark shifts¹⁰ and the Doppler width reduction from counterpropagating beams,¹¹ which are unique to the two-photon problem, are clearly demonstrated.

The experiment can be described using the simplified three-level system shown in Fig. 1. The sum of the input frequencies $\omega_1 + \omega_2$ is near resonant with the two-photon transition $|1\rangle \leftrightarrow |2\rangle$ with a frequency offset δ , which is much smaller than the intermediate-state frequency offset $\Delta \equiv \Omega_{n_2} - \omega_2$. The input field \mathcal{E}_1 , which is much stronger than \mathcal{E}_2 , is sufficient to shift the two-photon transition on resonance via the optical Stark effect. The nutation and FID signal is then detected by monitoring the weak beam \mathcal{E}_2 . Similar to their one-photon analogs, the two-photon nutation and FID effects can be visualized, using the vector model,⁴⁻⁶ as the precession of the two-photon polarization vector \vec{r} about the effective field $\vec{\gamma}$, namely, $d\vec{r}/dt = \vec{\gamma} \times \vec{r}$. (The notation is that of Ref. 6.) The precession frequency is given by the magnitude of the $\vec{\gamma}$ vector, whose components are

$\gamma_1 = -\kappa \mathcal{E}_1 \mathcal{E}_2$, $\gamma_2 = 0$, and $\gamma_3 = \delta + (\Delta E_1 - \Delta E_2)/\hbar$, where $\kappa = |p_{1n} p_{n2}| / 2\hbar^2 \Delta$ and $\Delta E_i = -|p_{in} \mathcal{E}_i|^2 / 4\hbar \Delta$, $i = 1, 2$, are the optical Stark shifts, and p_{1n} and p_{n2} are the transition dipole moments. Generally, the term nutation signifies the precession process when $|\gamma_1| \gg |\gamma_3|$ (i.e., on resonance) while the term FID is used when $|\gamma_3| \gg |\gamma_1|$ (off resonance). In the present experiment, the two-photon transition is shifted by the time-dependent \mathcal{E}_1^2 on resonance and then off resonance, and the nutation effect evolves smoothly into FID. The more general term, precession, will be used to describe the entire process. The signature of this precession process is thus the observation of the alternating absorption and emission of light at the characteristic precession frequency $(\gamma_1^2 + \gamma_3^2)^{1/2}$.

The two-photon transition used in the experi-

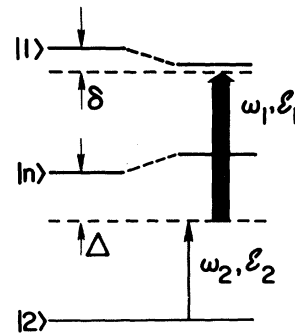


FIG. 1. Simplified three-level system for the two-photon resonance problem. \mathcal{E}_1 is assumed to be much stronger than \mathcal{E}_2 so that the optical Stark shift is entirely determined by \mathcal{E}_1 .

ment, the NH_3 transition $(\nu_2, J, K) = (0^-, 5, 4) \rightarrow (2^-, 5, 4)$, is nearly resonant with the sum of 10- μm CO_2 laser lines $P34$ and $P18$. The two-photon frequency offset δ has been accurately measured to be 294.37 MHz by Bischel, Kelly, and Rhodes,¹² and the offset Δ between the $P34$ line and the intermediate state $(1^+, 5, 4)$ has been determined to be 5250 MHz by Shimizu.¹³ Thus the requirement that Δ be large compared to δ is satisfied. The two input waves propagated in opposite directions to reduce the Doppler width to less than 2 MHz. As shown below, this is a necessary condition for the observation of the two-photon precession signal. The two beams were polarized parallel to one another so that the selection rule $\Delta M = 0$ applies. Thus, for each M sublevel, the only allowed transition is $(0^-, 5, 4, M) \rightarrow (2^-, 5, 4, M)$ with the uniquely defined intermediate state $(1^+, 5, 4, M)$. Note that since the system was initially 294 MHz away from resonance, one must rely on the optical Stark shift to bring the system to resonance. By the judicious choice of laser intensities and because of the M^2 dependence of the optical Stark shift, one could selectively bring *only* the degenerate $M = \pm 5$ states into resonance. Effects from all other M states could be neglected since they were at least 100 MHz, i.e., 50 times the residual Doppler linewidth, away. Thus, in the notation of Fig. 1, the states $|1\rangle$, $|n\rangle$, and $|2\rangle$ are $(\nu_2, J, K, M) = (2^-, 5, 4, \pm 5)$, $(1^+, 5, 4, \pm 5)$, and $(0^-, 5, 4, \pm 5)$, respectively. The dipole moments involved are thus uniquely defined and known¹²: $p_{1n} = 0.17$ D and $p_{2n} = 0.16$ D.

Experimentally, \mathcal{E}_1 was the $P18$ line from a grating-tuned CO_2 transverse-excitation atmospheric (TEA) laser (Tachisto Model 215G), operating in a single longitudinal mode by the addition of a low-pressure section inside the cavity.¹⁴ The 100-nsec output pulse was monitored by a fast photon-drag detector with a Tektronix 7904 scope. The \mathcal{E}_2 beam was from a longitudinally pulsed low-pressure (10 Torr) CO_2 laser at the $P34$ line. In the time scale of the experiment (100 nsec), \mathcal{E}_2 could be considered cw. The choice of a pulsed strong beam \mathcal{E}_1 and a cw weak beam \mathcal{E}_2 has two advantages. First, the time-dependent optical Stark shift is entirely determined by the strong beam. Second, the precession signal is easily observable on the weak beam since its magnitude is proportional to the field strength of the *strong* beam.^{4,6} Further, by making the weak beam nearly resonant to the transition between the ground and intermediate states and the strong beam nearly resonant to the transi-

tion between the intermediate and the final states, there can be little excitation in the intermediate state and parasitic one-photon resonant effects are effectively eliminated. Of course, to obtain a clean precession signal, it is necessary that the spatial intensity variation of the strong beam be minimized over the entire cross section of the weak beam. To this end, the strong beam passed through a 6-mm aperture, and the 10-cm-long NH_3 cell was put in the far-field region of the aperture. The weak-beam diameter was reduced to 2 mm, and intersected the central flat region of the strong beam. The intensities for the two beams in the cell were ~ 2 kW/cm² and 0.5–2 MW/cm². The weak beam, after propagating through the cell, was detected by a fast photoconductor (Ge:Cu at 4.2°K) and another 7904 scope, with an overall time constant of 2 nsec. The NH_3 pressure was monitored by a capacitive manometer (MKS Baratron).

A typical set of data is shown in Figs. 2(a) and

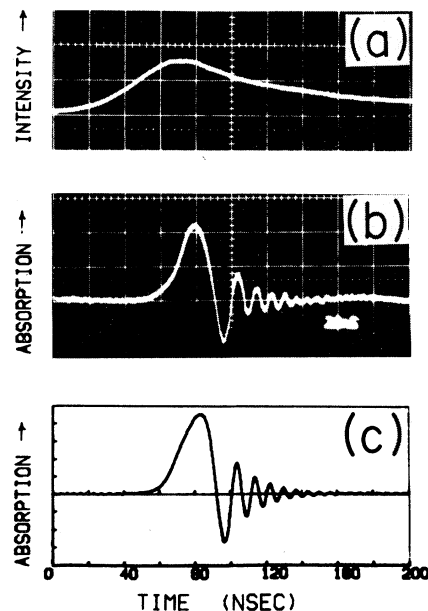


FIG. 2. (a) Single-mode TEA laser pulse detected by a high-speed photon-drag detector. Time scale, 20 nsec/div; vertical scale, 10 mV/div. (b) Simultaneous detection of the precession signal of the weak beam after passing through the 10-cm NH_3 cell at 150 mTorr. The alternating absorption and emission of light is the clear signature of the precession process. Time scale, 20 nsec/div; vertical scale, 10 mV/div. The weak-beam dc signal was -1.5 V. (c) Calculated two-photon precession signal, using the two-photon vector model and known experimental parameters. The TEA laser pulse in (a) was digitized and used as the input to the calculation. The result is plotted on the same scale as the oscilloscope traces.

2(b). The NH_3 pressure was 150 mTorr. The single-mode TEA laser pulse is shown in Fig. 2(a) and the precession signal on the weak beam is shown in Fig. 2(b), both at 20-nsec/div time scale. The characteristic precession signal, the alternating absorption and emission of light due to the precessing \vec{r} vector, is evident in Fig. 2(b). Note the interesting feature that the precession frequency increased with time, with the precession period decreasing from ~ 20 to ~ 5 nsec. This is easily understood in terms of the vector model. The precession frequency $|\dot{\gamma}| = (\gamma_1^2 + \gamma_3^2)^{1/2}$ is a function of the optical Stark shift. Since the precession signal was observed at the trailing edge of the TEA laser pulse, the precession frequency increased with time as the system shifted away from resonance as a result of the decreasing optical Stark shift accompanying the decreasing laser intensity. Note also that the observation of the precession periods would have been impossible without the Doppler width reduction since these periods were much longer than the normal T_2^* of a few nanoseconds. As expected, the time dependence of the precession signal was independent of the field strength of the weak cw beam \mathcal{E}_2 , only the magnitude of the signal being linearly proportional to \mathcal{E}_2 . On the other hand, the precession signal was critically dependent on the pulse shape and peak intensity of the TEA laser pulse. Figure 2 corresponds to the case where at the peak of the pulse the molecules were brought exactly on resonance. A mere 5% reduction of the TEA laser power caused the precession signal to decrease by a factor of 3, indicating that the optical Stark shift fell short of bringing the system on resonance. On the other hand, when the input power was increased so that the molecules were brought through resonance once on the leading edge and again on the trailing edge of the pulse, two sets of precession signals appeared. Since the power level in Fig. 2(a) gave the cleanest precession signal, it will be used for the comparison with theory. It should be pointed out that the observed decay time of the precession signal was shorter than the 35-nsec collisional relaxation time T_2 for this pressure.¹² This was due to the finite spatial variation of \mathcal{E}_1 (about $\pm 1\%$ over the interaction region) that induced polarizations that would go out of phase in a time shorter than T_2 .

An important advantage of the $\text{NH}_3\text{-CO}_2$ system used in the experiment is that *all* parameters relevant to the two-photon vector model⁴⁻⁶ are

known. The quantities with the most uncertainties were the absolute laser field strengths in the interaction region, especially \mathcal{E}_1 which was not known to better than 20% in the experiment. However, from the critical dependence of the precession signal strength on the peak power, for the case above, \mathcal{E}_1 can simply be set so that the maximum optical Stark shift ΔE_1 is -294 MHz, bringing the molecules on resonance at the pulse peak. Knowing p_{1n} and ΔE_1 , the peak intensity of the \mathcal{E}_1 beam was calculated to be 0.92 MW/cm², well within 20% of the experimentally estimated value of 1 MW/cm². The pulse shape in Fig. 2(a) was digitized and used as the input to the numerical solution of the two-photon vector model, with the collisional relaxation time $T_2 = 35$ nsec, and the spatial variation of \mathcal{E}_1 assumed to be $\pm 1\%$ over the interaction region. The calculated precession signal, plotted on the same time scale as the oscilloscope traces, is shown in Fig. 2(c). The agreement between theory and experiment is quite remarkable and demonstrates the usefulness and power of the two-photon vector model. Calculation has also been carried out assuming perfectly uniform \mathcal{E}_1 . The result was almost identical to Fig. 2(c) except for a longer signal decay time.

Data have been obtained at other pressures. In agreement with the two-photon linewidth of 28 MHz/Torr measured by Bischel, Kelly, and Rhodes,¹² the collisional relaxation time became dominant at ~ 400 mTorr and the precession signal became increasingly difficult to observe for further pressure increases.

In conclusion, this is the first experimental observation of the two-photon analog of a familiar one-photon precession process. It demonstrates the importance of effects such as the optical Stark shifts that are special to the two-photon problem. The excellent agreement with the prediction of the two-photon vector model provides the first quantitative confirmation of the model, and clearly points to the possible observations of other two-photon coherent effects such as self-induced adiabatic rapid passage,¹⁵ adiabatic following, and photon echoes.

It is my pleasure to thank D. R. Grischkowsky for fruitful discussions on the two-photon problem from which many ideas and techniques in this work were developed, and J. A. Armstrong and J. J. Wynne for their critical reading of the manuscript. The skillful technical assistance of P. A. Roland is gratefully acknowledged.

¹For a discussion of one-photon coherent effects, see, for example, L. Allen and J. H. Eberly, *Optical Resonance and Two-Level Atoms* (Wiley, New York, 1975). References to earlier NMR work can be found in A. Abragam, *The Principle of Nuclear Magnetism* (Oxford Univ. Press, Oxford, England, 1961).

²S. R. Hartman, IEEE J. Quantum Electron. **4**, 802 (1968).

³E. M. Belenov and I. A. Poluektov, Zh. Eksp. Teor. Fiz. **56**, 1407 (1969) [Sov. Phys. JETP **29**, 754 (1969)].

⁴M. Takatsuji, Phys. Rev. A **11**, 619 (1975).

⁵R. G. Brewer and E. L. Hahn, Phys. Rev. A **11**, 1614 (1975).

⁶D. Grischkowsky, M. M. T. Loy, and P. F. Liao, Phys. Rev. A **12**, 2514 (1975).

⁷R. L. Shoemaker and R. G. Brewer, Phys. Rev. Lett. **28**, 1430 (1972).

⁸N. Tan-no, K. Yokoto, and H. Inaba, Phys. Rev.

Lett. **29**, 1211 (1972).

⁹M. Matsuoka, H. Nakatsuka, and J. Okada, Phys. Rev. A **12**, 1062 (1975).

¹⁰P. F. Liao and J. E. Bjorkholm, Phys. Rev. Lett. **34**, 1 (1975).

¹¹L. S. Vasilenko, V. P. Chebotaev, and A. V. Shishaev, Pis'ma Zh. Eksp. Teor. Fiz. **12**, 161 (1970) [JETP Lett. **12**, 113 (1970)].

¹²W. K. Bischel, P. J. Kelly, and C. K. Rhodes, Phys. Rev. A **13**, 1829 (1976).

¹³F. Shimizu, J. Chem. Phys. **52**, 3572 (1970).

¹⁴A. Gondhalekar, E. Holzhauser, and N. R. Heckenberg, Phys. Lett. **46A**, 229 (1973). Very useful information on the single-mode operation of the TEA laser has also been provided by R. L. Aggarwal, N. Lee, and C. Chase (private communication).

¹⁵D. Grischkowsky and M. M. T. Loy, Phys. Rev. A **12**, 1117 (1975).

Observations of Collective Ion Acceleration by a Relativistic Electron Beam in a Magnetic Cusp*

C. W. Roberson, S. Eckhouse, A. Fisher, S. Robertson, and N. Rostoker

Physics Department, University of California, Irvine, California 92717

(Received 2 March 1976)

We have observed ion pulses of 10^{13} protons by passing hollow relativistic electron beams through a magnetic cusp. Ion pulses are observed with drift-chamber fill pressures from 75 to 600 mTorr of H_2 . Magnetic fields of 0.8 kG suppress the mechanism responsible for acceleration without magnetic field. A different mechanism appears to turn on and peaks as the cusp threshold is approached. More than 10^{11} protons with energies greater than 2 MeV are observed.

In conventional particle accelerators, the electric and magnetic fields at the particle are produced externally and are subject to limitations imposed by $\nabla \times \vec{E} = 0$ and $\nabla \cdot \vec{E} = 0$ in addition to the usual technical limitations of electrical breakdown. In a collective accelerator the electromagnetic fields that accelerate a particle are internal and produced by many charged particles. The magnitude of the internal field is determined mainly by the beam density that can be achieved.

The first observations of collectively accelerated ions with intense electron beams were in the experiment of Graybill and Uglum.¹ They injected a 1.6-MeV, 40-kA beam into a drift chamber filled with 200 mTorr of hydrogen and observed 100 A of 5-MeV protons. The electric field was about 100 MV/m which is a factor of 10 greater than in conventional accelerators. However, the acceleration took place over a distance of only 5 cm. In conventional accelerators the design and control of the fields at the particle is a highly developed science. In collective accelerators,

since the fields are internal and created by many particles, the problem of design and control is still at a very early stage and involves much more complicated physics. One of the few methods available for design and control of the electron beam is the application of an externally produced magnetic field. In previous experiments this suppressed the collective acceleration.² We report new experiments where collective acceleration is enhanced by an external magnetic cusp.

Collectively accelerated ions have been observed in a number of experiments¹⁻¹⁰ when an intense beam is propagated through a low-pressure gas without an external magnetic field. There has been considerable theoretical effort in conjunction with these experiments.¹¹⁻¹³ The experimental results are usually interpreted in terms of the acceleration of the space-charge well at the head of the beam as it breaks down the neutral gas or in terms of a localized pinch.

Figure 1 is a sketch of the apparatus. The electron-beam generator produced a 1.3-MeV,

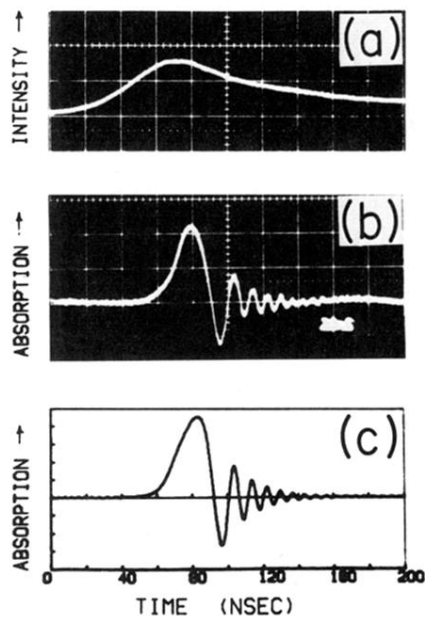


FIG. 2. (a) Single-mode TEA laser pulse detected by a high-speed photon-drag detector. Time scale, 20 nsec/div; vertical scale, 10 mV/div. (b) Simultaneous detection of the precession signal of the weak beam after passing through the 10-cm NH_3 cell at 150 mTorr. The alternating absorption and emission of light is the clear signature of the precession process. Time scale, 20 nsec/div; vertical scale, 10 mV/div. The weak-beam dc signal was -1.5 V. (c) Calculated two-photon precession signal, using the two-photon vector model and known experimental parameters. The TEA laser pulse in (a) was digitized and used as the input to the calculation. The result is plotted on the same scale as the oscilloscope traces.